J. Water Environ. Nanotechnol., 3(3): 235-242 Summer 2018

ORIGINAL RESEARCH PAPER

The flexible route for the electrosynthesis of visible light active $Cd_xZn_{1-x}O$ nanostructures by sequential anodic dissolution of metallic electrodes

Saied Saeed Hosseiny Davarani[1], Hamid Reza Moazami[2]*, Taher Yousefi[3], Masoud Abrari[4]

[1] Faculty of Chemistry, Shahid Beheshti University, Tehran, Iran
[2] School of Physics and Accelerators, Nuclear Science and Technology Research Institute, Tehran, Iran
[3] Materials and Nuclear Fuel Research School, Nuclear Science and Technology Research School, Tehran, Iran
[4] Laser and Plasma Research Institute Shahid Beheshti University, Tehran, Iran

Received: 2018.05.11 Accepted: 2018.07.01 Published: 2018.07.30

ABSTRACT

A flexible route for the electrosynthesis of visible light active $Cd_xZn_{1-x}O$ nanostructures has been proposed. Various nanostructures were prepared by anodic dissolution in 0.1M Me_4NCl by using an applied potential of 15V for 30min. The prepared nanostructures were characterized by diffuse reflectance UV-Vis spectroscopy (DRS), Fourier transforms infrared spectrometry (FT-IR), X-Ray diffraction (XRD) and scanning electron microscopy (SEM). The results showed that the crystalline structure, morphology, and energy band gap of the products can be finely adjusted only by varying the duty cycle of the anodeswitching. The visible light activity of the obtained nanostructures was investigated using methyl orange as a model organic pollutant. It was found that the proposed method can be used to obtain very effective $Cd_xZn_{1-x}O$ photocatalysts by fine tuning of the morphology and energy band gap. The prepared photocatalyst retained 80% of its original activity after 5 replicated uses.

Keywords: *Electrosynthesis, Anodic Dissolution, Cadmium-Zinc Oxide, Photocatalyst, Visible Light*

How to cite this article
Saeed Hosseiny Davarani S, Moazami HR, Yousefi T, Abrari M. The flexible route for the electrosynthesis of visible light active $Cd_xZn_{1-x}O$ nanostructures by sequential anodic dissolution of metallic electrodes. J. Water Environ. Nanotechnol., 2018; 3(3): 235-242. DOI: 10.22090/jwent.2018.03.004

INTRODUCTION

ZnO is known as an II-VI semiconductor with a wurtzite crystal structure and an energy band gap of 3.37 eV at room temperature[1]. ZnO nanostructures have already been extensively investigated for photocatalytic degradation of organic pollutants because of their high activity, biocompatibility and good chemical and mechanical stability[2]. In this process, ZnO is illuminated by incident photons with energy level higher than its band gap energy resulting in excitation of the electrons (e^-) from the valence band to the conduction band with subsequent holes (h^+) production in the valence band. The photo-generated holes react with either water (H_2O) or hydroxyl ions ($OH^•$) adsorbed on the catalyst surface to produce hydroxyl radicals (OH^-) and the photogenerated electrons react with oxygen (O_2) to form superoxide ions ($O_2^{•-}$) (). As a result, the decomposition of the organic materials can be achieved by their reaction with these radicals[3]. High energy band gap of ZnO restricts its photocatalytic activity in the UV region. Various techniques have already been employed for band gap tuning of ZnO to make it active within the visible region [4]. In recent works, CdS[5], CNT[6], and carbon[7] has been introduced to the ZnO matrix to inducephotocatalytic activity under the visible light. Furthermore, the coupling of ZnO with narrow band gap semiconductors has been employed as a

* Corresponding Author Email: *hamrezmoa@yahoo.com*

helpful technique to shift the photocatalytic activity of ZnO toward the visible region. Cadmium oxide (CdO) is a n-type semiconductor with a direct band gap of 2.5 eV; therefore, the band gap of ZnO could be tuned by CdO alloying. Various methods including solvothermal[8], electrospinning[9], electrochemical deposition[10], and sol-gel[11] have already been reported for the preparation of ZnO-CdO alloy. The present work discusses the synthesis of $Cd_xZn_{1-x}O$ nanostructures by sequential anodic dissolution method. The prepared samples are characterized by different techniques and are used for the photodegradation of methyl orange under visible light. In this study, we compared the photocatalytic activity of$Cd_xZn_{1-x}O$ (x= 0.10,0.20,0.30,0.40,0.50) nanoparticles by using methyl orange (MO) dye as a model organic pollutant under visible light. Through these experiments, the influence of the amount of Cd on the photocatalytic performance of the nanoparticles was investigated. The fabricated nanoparticles were characterized using a variety of analytical methods, including field emission scanning electron microscopy (FE-SEM), X-ray diffraction (XRD), diffuse reflectance spectroscopy (DRS) and UV-Visible spectroscopy.

EXPERIMENTAL

Chemicals and reagents

Me_4NCl was purchased from Merck (Darmstat, Germany) and was used without further purification. Two cylindrical electrodes of zinc metal and cadmium metal (purity of 99%) with a diameter of 1 cm and a height of 10 cm were purchased from Merck. All solutions were prepared with deionized water prepared through an Absaz water purification system (Tehran, Iran). The specifications of the prepared water are presented in Table 1.

Electrosynthesis

Two cylindrical electrodes of zinc metal and cadmium metal were used as sacrificial anodes with a diameter of 1 cm and a height of 10 cm. The sacrificial anodes were placed on both sides, 1cm apart from a steel 316L planar electrode working as the cathode. Initially, the electrodes had been wiped out of possible contaminations by sonication in ethanol and deionized water. An aqueous solution of 0.1M Me_4NCl salt was utilized as both supporting electrolyte and stabilizer under stirring and thermostatic conditions (at 60˚C). The electrosynthesis was carried out by applying a constant potential of 15V for 30 min. An electronic circuitry was used to switch the electric potential between the interchangeable anodes. Five samples with different cadmium contents were prepared by adjusting the duty cycle of the anode switching. The anode switching was carried out by means of

Table 1. The pH and conductivity of the deionized water used for the preparation of $Cd_xZn_{1-x}O$ nanostructures

pH	Conductivity
5.9	0.15 µScm^{-1}

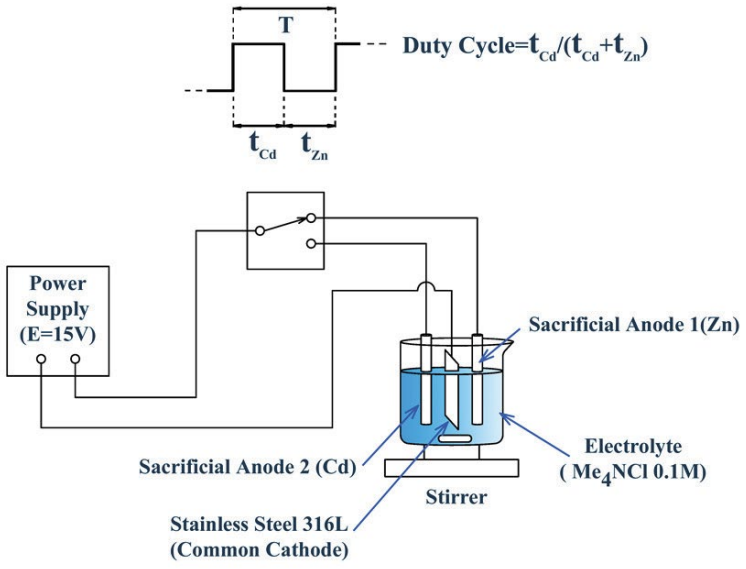

Fig. 1.Schematic diagram of the experimental setup.

a particular electronic circuit comprehensively described in our previous works [12-15].

A few minutes after the application of voltage, the solution turned milky due to co-precipitation of anodically dissolved Zn/Cd ions. After completion of the reaction, the obtained suspension was washed three times with water and ethanol. This precipitate was separated from the solution by centrifugation and washed with distilled water three times. The resultant precipitate was dried in an oven at 60 C° for 6 hr and further calcinated at 450 C° for 4 hrs. Fig. 1 shows the schematic diagram of the experimental setup.

Characterization

The morphology of the obtained nanostructures was studied by means of a TESCAN VEGA3-SB scanning electron microscope. The phase and crystallinity were characterized using STOE XD-3A X-ray diffractometer with Cu Kα radiation at λ=1.54056 A˚. The photodegradation kinetics was spectrophotometrically determined by means of a Shimadzu UV-2100 spectrometer. DRS of the samples were recorded by means of an Ava Spec-2048TEC spectrometer.

Photocatalytic activity measurements

The photocatalytic activity of $Cd_xZn_{1-x}O$ nanostructures was examined by measuring the rate of MO degradation in aqueous solution under visible light irradiation. The experiments were carried out in 50 mL beaker was filled with 15 mL of 10^{-5} M MO and 6 mg of $Cd_xZn_{1-x}O$ nanoparticles. Prior to the irradiation, the solution was kept in a dark place for 60 min to obtain adsorption-desorption equilibrium and the concentration of the solution was determined as initial concentration (C_0) of the dye solution. The solution was illuminated by a light source with a power of 80 lux and source-sample distance of 18 cm. The concentrations of MO in the solution were monitored and analyzed by applying the Beer-Lambert equation and measuring the absorbance at 664 nm using a UV-vis spectrophotometer.

RESULTS AND DISCUSSION

Electrosynthesis mechanism

The electrosynthesis of nanomaterials by anodic dissolution has been described in the literature [16, 17]. In this method, a metallic electrode undergoes anodic electrooxidation at sufficiently positive potential as the following equation:

$$M_{(s)} \rightarrow M^{n+} + ne^- \quad (1)$$

The electrogenerated metallic cation reacts with the hydroxyl ions initially present in the solution to obtain a metal hydroxide precursor:

$$M^{n+} + nOH^- \rightarrow M(OH)_n \quad (2)$$

The quaternary ammonium salt acts as a mild source of hydroxyl ions and the capping agent which prevents aggregation of the produced metal hydroxide nuclei. The latter action is crucial to obtain fine nanoparticles.

In this work, the anodic potential is sequentially applied to Zn and Cd electrodes. During t_{Cd}, when the potential is applied to the Cd electrode, the latter is anodically oxidized to Cd^{2+}:

$$Cd_{(s)} \rightarrow Cd^{2+} + 2e^- \quad t_{Cd} \quad (3)$$

$$Zn(s) \rightarrow Zn^{2+} + 2e^- \quad t_{Zn} \quad (4)$$

Similarly, the Zn electrode dissolves to Zn^{2+}during t_{Zn}:

The dissolved Cd^{2+} and Zn^{2+}cations react with hydroxyl ions to obtain a mixed hydroxide precursor that loss water to make the final product.

$$(1-x)Zn^{2+} + xCd^{2+} + yOH^- \rightarrow Cd_xZn_{1-x}(OH)_y \quad (5)$$

Crystal structure

XRD patterns of $Cd_xZn_{1-x}O$ composites are shown in Fig. 2. The X-ray diffraction peaks of ZnO can be attributed to the hexagonal wurtzite phase of (ICDD card No.: 79-0208) and also the lattice constant values of a = b = 0.326 nm and c = 0.521 nm. However, in XRD patterns of the $Cd_xZn_{1-x}O$ composites, two phases are observed with the significant broadening of wurtzite ZnO peaks. One is the hexagonal structure of ZnO and another is a cubic structure of CdO with peaks (111), (200), (211) and (220) (Card No. 73-2245) and lattice constant values a = b = c = 0.470 nm. The average crystallite size could be evaluated from the base peak according to Debye-Scherrer equation ($D = 0.891\lambda/\beta\cos\alpha$); where D is average grain size,λ the X-ray wavelength (0.1540 nm) and α and β are the diffraction angles and full width at half-maximum, respectively). The average particle size values were found to be 16.15, 28.85, 31.70, 45.12 and 57.21nm for various $Cd_xZn_{1-x}O$ nanostructures with x=0.1, 0.2.0.3, 0.4 and 0.5, respectively.

Diffuse reflectance spectroscopy

The UV-visible diffuse reflectance spectra of the$Cd_xZn_{1-x}O$ composites with different compositions in the wavelength range of 300–700 nm are shown in Fig. 3. All the prepared samples show absorption in the visible region. It can also be observed that there is a slight shift in the absorption edge as the x (the content of CdO) in the composite increases. Compared with the optical absorption of bare ZnO (~403 nm), $Cd_xZn_{1-x}O$ composite has two absorption edges [18]; the main edge due to ZnO and the second one due to CdO. The absorption edges for the $Cd_xZn_{1-x}O$ composite indicates that the photocatalytic activity of ZnO can be drawn toward the visible region by composite formation with CdO. Samples with a high amount of Cd (x=0.4 and 0.5) showed peak offsets between 400-600nm probably due to the formation of impurities. A possible impurity in the chloride-rich alkaline medium is CdOHCl [19].

Calculation of the band gap from diffuse reflectance

Taking into consideration the UV–visible absorption spectra and utilizing Tauc model (eq. 6), the optical band gap energy of the nanoparticle of $Cd_xZn_{1-x}O$ was calculated from Eq. 6[20]:

$$(\alpha h\nu)^2 = K(h\nu - E_g) \quad (6)$$

Where α is the absorption coefficient, hν the

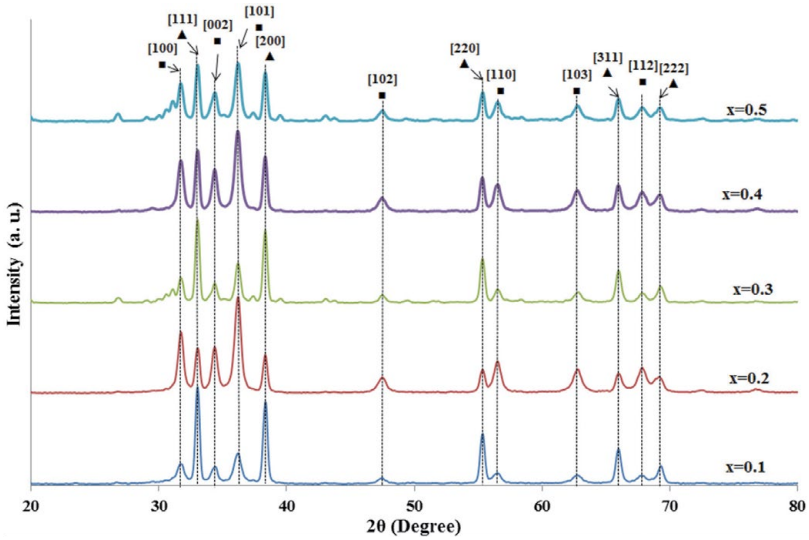

Fig. 2. X-ray diffraction pattern of different–ZnOsamples

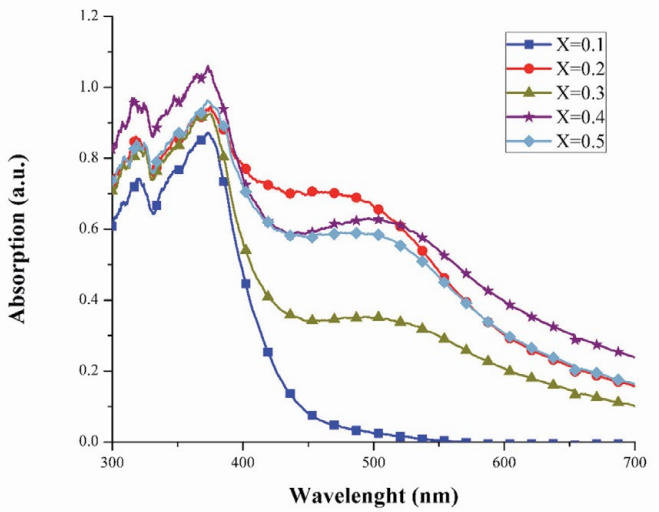

Fig. 3. UV-visible absorption spectra of the $Cd_xZn_{1-x}O$ composites with different compositions.

photon energy, K an invariant and E_g the band gap energy. Fig. 4 shows the plot of $(\alpha h\nu)^2$ *vs.* $h\nu$ while using the absorption data in which the extrapolated intercept provided the related E_g. To examine the consequence of CdO focus on a property of ZnO, we obtain different band gap energy by varying x which are summarized in Table 2. In accordance with our data analysis, band gap narrowing was observed by increasing the amount of Cd. It is well known that CdO is actually a low bandgap energy semiconductor, unlike ZnO, hence, it is expected that the band gap energy nanoparticle of the Cdo/ZnO must be of these types of materials (pure ZnO and CdO). Other researchers also reported band gap energy decline in the mixed ZnO and CdO composition in comparison with pure ZnO [21, 22].

Morphology

Fig. 5(a,b, c, d and e) show the surface morphology of $Cd_xZn_{1-x}O$ nanostructures with x= 0.1, 0.2, 0.3, 0.4 and 0.5, respectively. As can be seen, the morphology of the sample with x=0.1 (Fig. 5 (a)) comprises spherical nanoparticle with an average particle size of 23.4nm. The morphology of the nanostructure changed to interlocked nanosheets for the sample with x=0.2 (Fig. 5 (b)). The average diameter of the nanosheets was found to be 25.5 nm. The greater values of x resulted in the formation of a combination of nanosheets and nanoparticles morphology as demonstrated for x=0.3, 0.4 and 0.5 as Fig. 5 (c, d, e), respectively.

FT-IR

The as-synthesized $Cd_xZn_{1-x}O$ composites were further characterized by FT-IR spectrometry analysis. Fig .6displays the FT-IR spectra of ZnO and CdO–ZnO composites. The peak which is observed from 400 cm^{-1} to 600 cm^{-1} is attributed to the Zn-O bond vibrations of the particles [23]. The broad absorption band at ~3400–3500 cm^{-1} corresponds to the O-H stretching vibrations of water present in ZnO and CdO–ZnO[24] composites and other absorption bands at ~2916 cm^{-1} are assigned to the residual organic component [25]. Absorption at 1485 cm^{-1} showed characteristic absorption of the Cd-O bond.

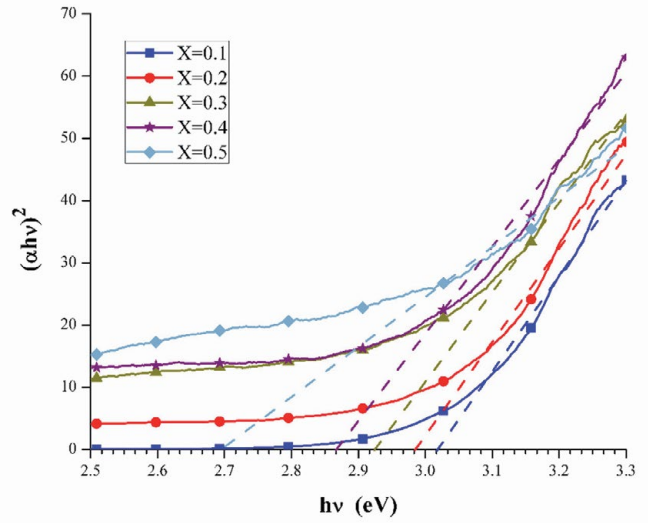

Fig. 4. The Tauc plot of different CdO–ZnO samples

Table 2. The average crystal size, band gap energy (E_g) and reaction rate constants (k) of MO photodegradation for different $Cd_xZn_{1-x}O$ samples

Sample name (nm)	Average crystal size (eV)	Band gap energy (Visible light)	K (min^{-1})
x=0.1	16.50	3.03	0.007
x=0.2	28.50	2.98	0.048
x=0.3	31.70	2.85	0.016
x=0.4	45.12	2.75	0.013
x=0.5	57.21	2.70	0.024

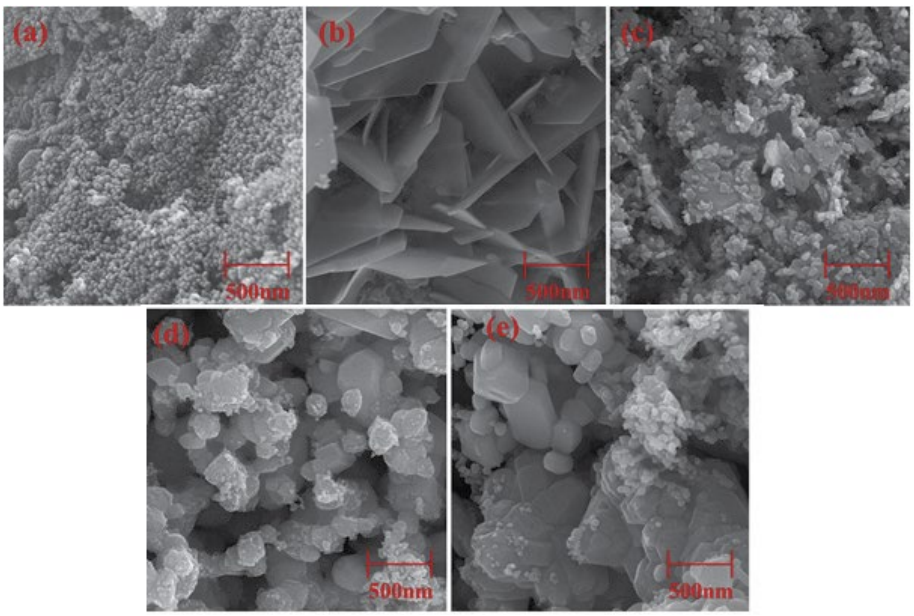

Fig. 5. FE-SEM images of different CdO–ZnO samples

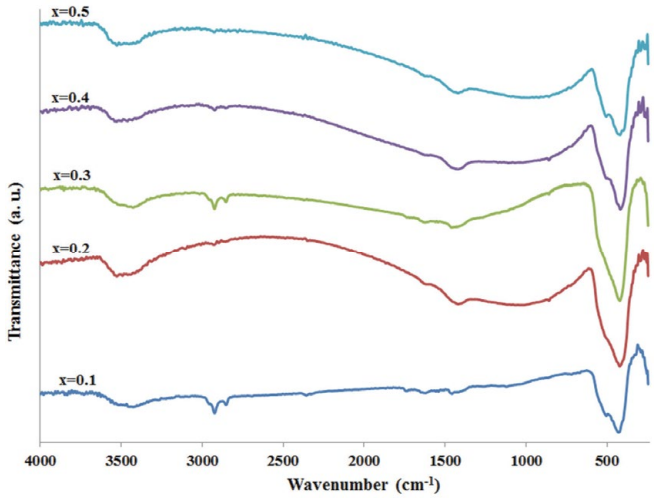

Fig. 6. FT-IR spectra of different CdO–ZnO samples

Photocatalytic activity

Methyl orange (MO) has often been used as a model organic pollutant for photocatalytic degradation study of semiconductors [26, 27]. The photocatalytic activity of the $Cd_xZn_{1-x}O$ nanoparticle was evaluated by measuring the rate of the degradation of MO dye under the visible light. The irradiation was performed for 120 min. It is well known that the photocatalytic degradation of MO is attributed to first order kinetics explained by the following equation [28]:

$$\ln (C_0/C) = kt \quad (7)$$

Where C_0 and C are the initial and time-dependent concentrations of MO, respectively. The $\ln(C_0/C)$ quantity was plotted as a function of irradiation time for various photocatalysts in Fig. 7. The linear behavior shows that the photocatalysis reaction follows the first order kinetics as described by Eq. 6. The reaction rate constants (k) from the slope of the linear fit were calculated (Table 1). Therefore, the MO degradation is principally assigned to the photocatalytic activity of the $Cd_xZn_{1-x}O$ nanoparticle. The photocatalytic activity enhancement was observed for x=0.2in comparison to other nanoparticles.

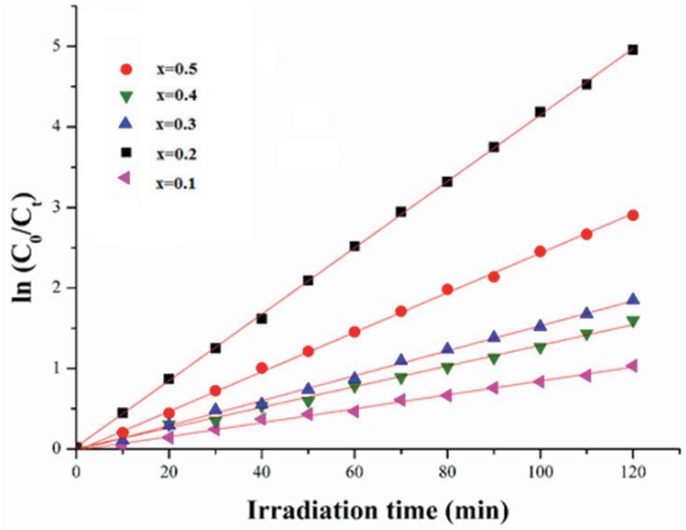

Fig. 7. Variation of $\ln(C_0/C)$ vs. irradiation time under the visible light on the $Cd_xZn_{1-x}O$ nanocomposites.

Further investigation of photocatalytic activity under visible radiation has also been performed for comparison. As discussed within the diffuse reflectance spectroscopy pure ZnO has no absorption in the visible region. Therefore, it has no photocatalytic activity under the visible radiation. The incorporation of Cd in the nanostructures improves the photodegradation kinetics This enhancement within the photocatalytic activity of $Cd_xZn_{1-x}O$ nanoparticles by CdO addition ($x\neq0$), relates to the band gap reduction that caused the absorption of visible radiation by the $Cd_xZn_{1-x}O$ nanoparticle. In order to achieve high photocatalytic activity under visible light, it is necessary to reduce the band gap of a semiconductor. On the other hand, lower energy band gap may increase the rate of recombination resulting in loss of the photocatalytic activity.

CONCLUSIONS

Photocatalysts are potential candidates in nanotechnology because of their promise in the conversion of solar power into chemical energy as well as in the degradation of numerous organic pollutants. The high energy band gap of common metal oxide semiconductors restricts their use as photocatalytic agents. The lowering of the energy band gap of semiconductors allows for greater efficiencies towards photocatalytic reactions. This is because the separation of photogenerated electron-hole pairs is increased by a hetero-junction between two semiconductors with matching electronic band structures. This heterojunction is important for the improved photocatalytic activity of the photocatalyst. The incorporation of CdO into the ZnO matrix led to band gap narrowing resulting in significant improvement of the photocatalytic activity under visible light. The highest visible light photocatalytic activity was observed for $Cd_xZn_{1-x}O$ with x=0.2. The decline in size and doping along with other suitable catalytic composites enhance the rate of the photocatalytic degradation of complex organic molecules. Sequential anodic dissolution is a facile route for the preparation of $Cd_xZn_{1-x}O$ nanostructures with a wide range of energy band gap and various morphologies. The produced nanoparticle of $Cd_x/Zn_{1-x}O$ can be utilized as an effective photocatalyst for organic materials degradation under visible light. In summary, the introduced CdO/ZnO may have good industrial applications in the field of wastewater treatment because of the less cost from the required activation energy (solar radiation), the fast and effective degradation of the organic materials as well as the negligible polluting the environment effect from the degradation reactions products (CO_2 and H_2O).

CONFLICTS OF INTEREST

The authors declare that there are no conflicts of interest.

REFERENCES

1. Lam S-M, Sin J-C, Abdullah AZ, Mohamed AR. Degradation of wastewaters containing organic dyes photocatalysed by zinc oxide: a review. Desalination and Water Treatment.

2012;41(1-3):131-69.
2. Sudha D, Sivakumar P. Review on the photocatalytic activity of various composite catalysts. Chemical Engineering and Processing: Process Intensification. 2015;97:112-33.
3. Sedghi R, Moazzami HR, Hosseiny Davarani SS, Nabid MR, Keshtkar AR. A one step electrospinning process for the preparation of polyaniline modified TiO 2 /polyacrylonitile nanocomposite with enhanced photocatalytic activity. Journal of Alloys and Compounds. 2017;695:1073-9.
4. Sedghi R, Nabid MR, Shariati M, Behbahani M, Moazzami HR. Preparation of PAN-based electrospun nanofiber webs containing Ni-ZnO as high performance visible light photocatalyst. Fibers and Polymers. 2016;17(12):1969-76.
5. Zirak M, Moradlou O, Bayati MR, Nien YT, Moshfegh AZ. On the growth and photocatalytic activity of the vertically aligned ZnO nanorods grafted by CdS shells. Applied Surface Science. 2013;273:391-8.
6. Samadi M, Shivaee HA, Zanetti M, Pourjavadi A, Moshfegh A. Visible light photocatalytic activity of novel MWCNT-doped ZnO electrospun nanofibers. Journal of Molecular Catalysis A: Chemical. 2012;359:42-8.
7. Samadi M, Shivaee HA, Pourjavadi A, Moshfegh AZ. Synergism of oxygen vacancy and carbonaceous species on enhanced photocatalytic activity of electrospun ZnO-carbon nanofibers: Charge carrier scavengers mechanism. Applied Catalysis A: General. 2013;466:153-60.
8. Ghosh M, Raychaudhuri AK. Structure and optical properties of Cd-substituted ZnO (Zn1−xCdxO) nanostructures synthesized by the high-pressure solution route. Nanotechnology. 2007;18(11):115618.
9. Yousef A, Barakat NAM, Amna T, Unnithan AR, Al-Deyab SS, Yong Kim H. Influence of CdO-doping on the photoluminescence properties of ZnO nanofibers: Effective visible light photocatalyst for waste water treatment. Journal of Luminescence. 2012;132(7):1668-77.
10. Li G-R, Zhao W-X, Bu Q, Tong Y-X. A novel electrochemical deposition route for the preparation of Zn1−xCdxO nanorods with controllable optical properties. Electrochemistry Communications. 2009;11(2):282-5.
11. Caglar Y, Caglar M, Ilican S, Ates A. Morphological, optical and electrical properties of CdZnO films prepared by sol–gel method. Journal of Physics D: Applied Physics. 2009;42(6):065421.
12. HosseinyDavarani SS, Moazami HR, Memarian E, Nojavan S. Electromembrane extraction through a virtually rotating supported liquid membrane. ELECTROPHORESIS. 2015;37(2):339-46.
13. Moazami HR, Nojavan S, Zahedi P, Davarani SSH. Electronic simulation of the supported liquid membrane in electromembrane extraction systems: Improvement of the extraction by precise periodical reversing of the field polarity. Analytica Chimica Acta. 2014;841:24-32.
14. Zahedi P, Davarani SSH, Moazami HR, Nojavan S. Surfactant assisted pulsed two-phase electromembrane extraction followed by GC analysis for quantification of basic drugs in biological samples. Journal of Pharmaceutical and Biomedical Analysis. 2016;117:485-91.
15. Mohammadi J, Davarani SSH, Moazami HR. Impedometric monitoring of the behavior of the supported liquid membrane in electromembrane extraction systems: An insight into the origin of optimized experimental parameters. Analytica Chimica Acta. 2016;934:98-105.
16. Abrari M, Ghanaatshoar M, Hosseiny Davarani SS, Moazami HR, Kazeminezhad I. Synthesis of SnO $$_2$$ 2 nanoparticles by electrooxidation of tin in quaternary ammonium salt for application in dye-sensitized solar cells. Applied Physics A. 2017;123(5).
17. Kazeminezhad I, Sadollahkhani A, Farbod M. Synthesis of ZnO nanoparticles and flower-like nanostructures using nonsono- and sono-electrooxidation methods. Materials Letters. 2013;92:29-32.
18. Krishnakumar B, Subash B, Swaminathan M. AgBr–ZnO – An efficient nano-photocatalyst for the mineralization of Acid Black 1 with UV light. Separation and Purification Technology. 2012;85:35-44.
19. Li Y, Wang Z, Ma X-d, Qian X-f, Yin J, Zhu Z-K. Large-scale CdX (X=S, Se) microtube arrays on glass substrate: transformation of CdOHCl microrod arrays by a simple template-sacrificing solution method. Journal of Solid State Chemistry. 2004;177(12):4386-93.
20. Ahmadi M, Asemi M, Ghanaatshoar M. Improving the electrical and optical properties of CuCrO2 thin film deposited by reactive RF magnetron sputtering in controlled N2/Ar atmosphere. Applied Physics A. 2018;124(8).
21. Ziabari AA, Ghodsi FE. Optoelectronic studies of sol–gel derived nanostructured CdO–ZnO composite films. Journal of Alloys and Compounds. 2011;509(35):8748-55.
22. Mosquera E, del Pozo I, Morel M. Structure and red shift of optical band gap in CdO–ZnO nanocomposite synthesized by the sol gel method. Journal of Solid State Chemistry. 2013;206:265-71.
23. Ansari AA, Kaushik A, Solanki PR, Malhotra BD. Nanostructured zinc oxide platform for mycotoxin detection. Bioelectrochemistry. 2010;77(2):75-81.
24. Moazami HR, Davarani SSH, Yousefi T, Darjazi H. Iron mediated cathodic electrosynthesis of hausmannite nanoparticles. Materials Science in Semiconductor Processing. 2015;38:240-8.
25. Arora K, Tomar M, Gupta V. Effect of processing parameters for electrocatalytic properties of SnO2 thin film matrix for uric acid biosensor. The Analyst. 2014;139(4):837.
26. Shang X, Li B, Zhang T, Li C, Wang X. Photocatalytic Degradation of Methyl Orange with Commercial Organic Pigment Sensitized TiO2. Procedia Environmental Sciences. 2013;18:478-85.
27. Ghule LA, Patil AA, Sapnar KB, Dhole SD, Garadkar KM. Photocatalytic degradation of methyl orange using ZnO nanorods. Toxicological & Environmental Chemistry. 2011;93(4):623-34.
28. Byrne C, Subramanian G, Pillai SC. Recent advances in photocatalysis for environmental applications. Journal of Environmental Chemical Engineering. 2018;6(3):3531-55.